

# Single Photon Counting with Silicon Photomultipliers, shortening systems and incoherent illumination

**J. M. Yebras**

[jmyebras@fis.ucm.es](mailto:jmyebras@fis.ucm.es)

**P. Antoranz**

**J. M. Miranda**

Dpto. Física Aplicada III, Facultad CC Físicas, Universidad Complutense de Madrid, Av. Complutense s/n, 28040, Madrid, Spain

Dpto. Física Aplicada III, Facultad CC Físicas, Universidad Complutense de Madrid, Av. Complutense s/n, 28040, Madrid, Spain

Dpto. Física Aplicada III, Facultad CC Físicas, Universidad Complutense de Madrid, Av. Complutense s/n, 28040, Madrid, Spain

In this work it is shown the benefit of using pulse shortening systems for conforming photodetection pulses provided by Silicon Photomultipliers (SiPMs). One of the main drawbacks when using SiPMs is the slow falling edge in the detection signal which can reach even hundreds of nanoseconds. Pulses obtained when using the shortening systems proposed here are single narrow peaks, with full width at half maximum (FWHM) around 10 ns, preserving the photonic modulation and with good pseudo-gaussian shape, single polarity and low ringing. Different tests are presented to illustrate the advantage of these systems in the detection of single photons emitted in short, incoherent pulses.

[DOI: <http://dx.doi.org/10.2971/jeos.2012.12014>]

**Keywords:** darkcounts, pulse shortening, single photon counting, SiPM

## 1 INTRODUCTION

Silicon Photomultipliers (SiPMs), also known as Geiger-mode Avalanche Photo-Diodes (GAPDs) are a new generation of semiconductor photodetectors that provide very high sensitivity and show several advantages as compared to more traditional devices (e.g. photomultipliers, PMTs) [1, 2]. SiPMs have small active area and exhibit optical cross-talk, but despite these limitations they feature outstanding qualities compared to other photodetectors such as high quantum efficiency, high internal gain and insensitivity to magnetic fields. These devices work at very low bias voltages (<100 V), show almost no aging and can be exposed fully biased to daylight without destruction [3]–[6].

The emergence of photonics applications requiring single photon detection has been driving significant technological advances during the last five years. Single photon sensitivity is a key enabler for photon-starved applications such as long range free-space communications and detectors for flash ladar 3D imaging. These applications are often best served by SiPMs, which can achieve high performance consistent with practical operating conditions and robust deployment. SiPMs also have direct application in fluorescence detection with biomedical purposes: single molecule detection [7], fluoro-labelled cells detection for flow cytometry [8], nuclear medicine [9, 10], radioimmunoassay, genic expression, study of biochemical cycles, etc. Furthermore, SiPMs can help to create the long sought scanner which combines PET and Magnetic Resonance, due their high quantum efficiency and insensitivity to magnetic fields [11]. Their reduced size can also lead them to replace PMTs in all portable gamma ray

monitors such as intra-operative hand-held gamma cameras or field radiometers.

Other technological fields can take benefit from these photon counting systems. The exploitation of the quantum properties of photons for quantum cryptography and other quantum information processing techniques, for instance, is critically dependent on single photon detection [12]. SiPMs have also found an emerging application field in astroparticle physics experiments [13]–[16]. Some recently published work demonstrates that SiPMs compete very well with PMTs for applications in which high photonic resolution is needed. New models, analysis tools and applications are being developed. For example, SiPM is being used for providing real-time dosimetry in mammography [17]. Other authors report models to express photon number resolution of the device in analytical form taking into account crosstalk and afterpulsing phenomena [18]. Ramilli et al propose tools to describe the operation of SiPM and to model darkcount and crosstalk processes, which are based on Single Photon Counting (SPC) patterns [19].

The SiPM is a matrix device where each cell is an avalanche photodetector (APD) working in Geiger mode that includes a quenching resistor [3, 4], [20]. That resistor is in charge of collapsing the avalanche process in each single APD a short time after it starts. As all the cells in the device are connected to a common metallic grid, the total photocurrent is proportional to the number of incident photons (that is, to the number of fired cells). SiPM photosignal is modulated in amplitude, that

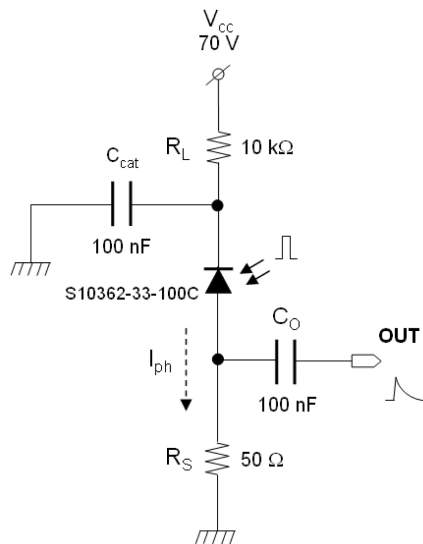


FIG. 1 SiPM bias circuit.

is, the amplitude of the photodetection signal is directly proportional to the intensity of the exciting pulse [4]. The typical response of the SiPM to an incoming exciting pulse is a very fast rising edge at the time the avalanche is produced followed by a slow downfall when the avalanche is quenched [4], [6]. This pulse shape is observed even for short exciting pulses ( $< 10$  ns). In the present work it is shown the potential of photodetection pulse shortening systems for improving SPC patterns using large active area SiPMs. Two different pulse shortening techniques have been used. The first one is based in a reflectometric scheme where a short-circuited stub provides an inverted and delayed version of the original signal. The combination of both signals results in an output pulse narrower than the original. In the second scheme the short-circuited stub is replaced by an analog subtractor circuit. One of the incoming signals to the subtractor is a delayed version of the other one if the photosignal is divided and a delay is applied to one of the resulting signals.

## 2 SETUP DESIGN

The measurements were made using two different SiPMs: S10362-33-100C, with an active area of  $3\text{ mm} \times 3\text{ mm}$  [21], [22] and S10362-11-050C, with an active area of  $1\text{ mm} \times 1\text{ mm}$  [23]. The bias circuit was designed according to its manufacturer recommendation and can be seen in Figure 1.  $R_L$  is a limiting resistor for guarding the device,  $R_S$  is the photocurrent sensing resistor and  $C_O$  is a blocking capacitor whose aim is to remove any DC component in the signal. The biasing voltage is provided by the high accuracy power source Keithley model 6487 [24].

Because of our objective is to provide a weak optical illumination to the SiPM in a simple way, the excitation pulse is obtained by feeding several LED models with the function generator Tektronix AFG3252 (2 GS/s, 240 MHz). Two main LED models were used in experiments; first, the ultraviolet LED model HUVL400-5x0B (Hero Electronics) with the following specifications: central emission wavelength at 400 nm, close to the maximum Photo-Detection Efficiency (PDE) of SiPMs

(located at about 450 nm), spectral bandwidth of 20 nm, output power up to 2.2 mW and half intensity angle of  $\pm 20$  degrees [25]; second, the red AlGaInP laser diode ADL-65074TR (Laser Components) operated in LED mode, whose central emission wavelength is located at 655 nm [26]. Single Photon Counting patterns shown in this work demonstrate that the typical Poisson-type distribution for impinging photons have been achieved by using these sources. The wavelength range for the emission of the light source has not resulted critical. Furthermore, non-controlled and frequency-induced parasitic phenomena in LEDs are unlikely because of the low optical repetition frequency used in the experiments (typically 100 kHz). LED and SiPM are connected through an optical fibre using plastic hoods for assuring mechanical fit and providing luminous isolation. A deeper luminous isolation of the SiPM (for reducing as much as possible background events) is achieved covering the whole SiPM bias board with several layers of black cloths.

Since the SiPM pulse amplitude is in the order of millivolts, several gain stages have been used in order to obtain enough amplification (44 dB nominal). For the first stage it was selected the MMIC amplifier model BGA616 (Infineon Technologies [27]) whose bias network is according to previous works in our group [28, 29]. Experimental measurements provide a gain factor around 16 dB and a noise figure of 3.8 dB. Two commercial pulse amplifiers complete the gain chain (Figure 2). These are ZPUL-21 (inverting, gain factor of 10 dB for experimental measurements ranging from 10 kHz to 700 MHz [30]) and ZPUL-30P (non-inverting, gain factor of 31 dB for experimental measurements ranging from 10 kHz to 700 MHz [31]), both from Mini-Circuits. Attenuators have been inserted between elements in the system to improve the impedance matching, reduce the ringing between stages and match the amplitude levels to the amplifying stages.

Figure 3 shows the two shortening schemes previously explained in the introductory section. They both provide a certain loss in the amplitude of the photosignal. However, this is not a major inconvenient because the proportionality of the amplitude with the optical excitation is preserved and because the amplitude can be restored to higher values with extra amplification or by including the shortening subsystem in the middle of the gain chain. The operational amplifier LM7171 was selected for the subtractor circuit due to its very high speed operation (slew rate  $\sim 4100\text{ V}/\mu\text{s}$ ) [32]. The delay could be obtained either through a splitter with arms of different lengths (which produces the best results), or through a splitter with arms of equal lengths and a delaying device (opamp in buffer mode) in one of the arms. A Schottky diode could be used at the end of the processing chain. This diode could conform the pulse shape by removing negative tails. Several models of Schottky diodes were tested, obtaining the best results with the model BAT17, which exhibits a very low turn on voltage and therefore has no relevant effects on the linearity for weak signals [33]. However, for SPC experiments is not essential and it was not used.

For tracing the SPC patterns, two ways were explored. The high frequency digital oscilloscope Agilent Infiniium DSO81204B (12 GHz, 40 GSa/s) allows to trace and save

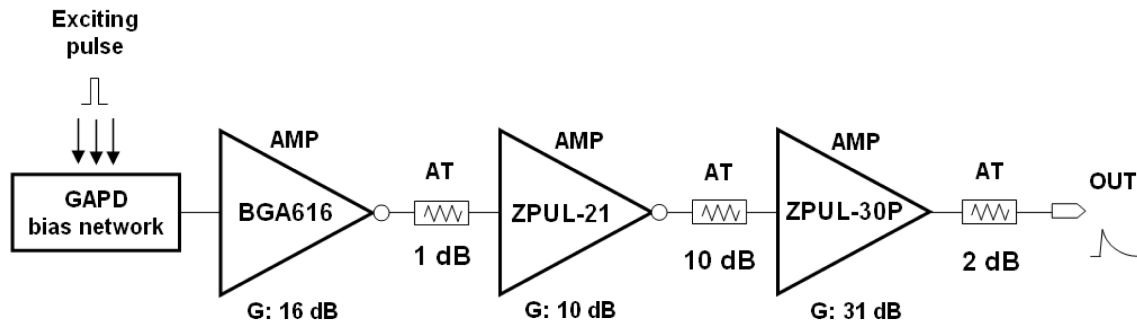


FIG. 2 Gain chain used in the experiments (44 dB nominal). The GAPD bias network is an integrated circuit which includes both the photodetector and its bias network.

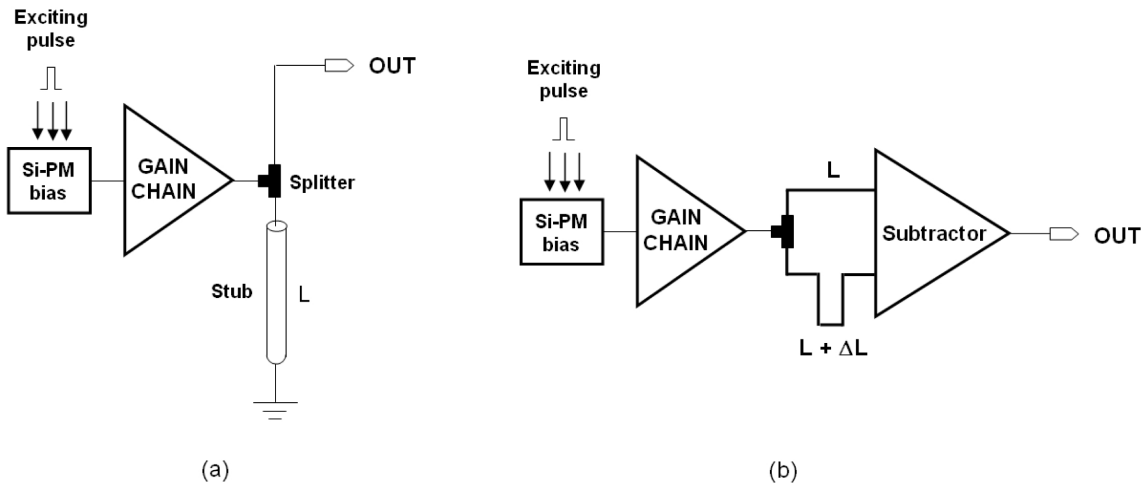


FIG. 3 Pulse shortening system based on reflectometry (a) and on subtractor feeded with inputs of different lengths (b).

amplitude histograms [34]. The histogram utility works like a multichannel analyzer. In the other option, a Matlab program was developed for calculating SPC patterns from event counts. The program calculates, for each event, the peak voltage or the charge of the signal and histograms based on signal maxima or charge integration are traced. Both options provide good results, but the first one was selected by clear reasons: time for tracing the SPC is much shorter than with Matlab option, it is possible to observe real-time the formation of the pattern and no extra computational charge or manipulation of large amount of data files are needed. For better observing the pulses and SPC the oscilloscope bandwidth was reduced to 1 GHz. Also, patterns were processed with a mobile mean tool for making them less noisy.

### 3 EXPERIMENTAL RESULTS

Figure 4 shows that it is hard to obtain clear SPC patterns by applying only high gain (44 dB nominal) to photodetection pulses. Pattern is affected by a strong base distribution caused by the excess noise in the SiPM and by secondary effects in the device, like crosstalk and darkcounts, resulting that photo-peaks are poorly defined (low differences between peaks and valleys). Often, it is not even possible to reach this weak result and it is obtained a distribution with a Poisson-type profile but with no distinguishable peaks.

Filtering the photodetection signal (for the result shown in

Figure 5, it was used a passive band-pass filter with cutoff frequencies of 60 MHz and 230MHz) it is possible to enhance the pattern, being able to distinguish up to five peaks. Also, distances peak-valley reveal a better Poisson-type distribution imputable to the type of exciting illumination. However, peaks remain mounted on a large mountain that makes difficult to establish clear thresholds for separating between the arrival of  $n$  and  $n \pm 1$  photons.

As it is shown in Figure 6, the use of the reflectometric shortening scheme, even with low gain (16 dB, only BGA616 amplifier) provides better results than before. An example of the photodetection signal shortening can be seen in Figure 11(a) for a higher gain factor. Patterns shown in Figure 6 reveal a Poisson distribution, as it was expected [19]. When exciting pulse amplitude is near the limit for direct LED excitation (Figure 6-gray) the pattern shows up to six clearly distinguishable peaks in a Poisson-type configuration. When the exciting pulse is slightly higher (1 %, Figure 6-black) the pattern, as it was expected, is significantly distorted: the mean of the pattern is shifted to higher voltages, height of peaks tends to a Gauss-type configuration, more peaks appear and base distribution is greater. Note that the distance between peaks in Figure 6 is roughly 1 mV. This extremely low value suggests the use of additional gain stages, so that amplitude thresholds corresponding to different number of arriving photons can be clearly resolved, and channels in a single photon counter can be easily set.

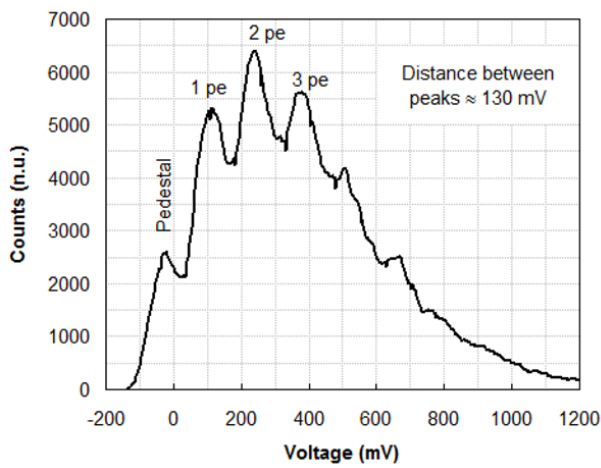


FIG. 4 SPC pattern obtained with high gain (44 dB nominal) and with no pulse shortening system. SiPM model S10362-33-100C (3 mm x 3 mm). Biasing voltage: 70 V. Incoming excitation pulses with width of 10 ns and wavelength of 400 nm.

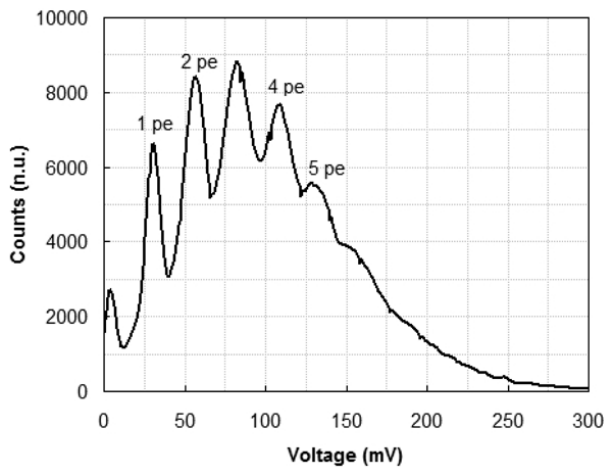


FIG. 5 SPC pattern obtained by mean of band-pass passive filtering (bandpass: 60 MHz-230 MHz). SiPM model S10362-33-100C (3 mm x 3 mm). Biasing voltage: 70 V. Incoming excitation pulses with width of 10 ns and wavelength of 400 nm.

One could think that an alternative to higher gain in the processing chain would be to enhance the intrinsic gain of the SiPM (i.e.: multiplication factor) by increasing its biasing voltage. However, it is not so good idea. As it can be seen in Figure 7, it is true that even with a slight increase in biasing voltage it is possible to separate significantly the peaks in the pattern, but it also happens that peaks are wider (because the excess noise factor in SiPM is directly related with intrinsic gain) and the influence of darkcounts and false fires is much greater. When it is provided an excess voltage (voltage above the breakdown voltage of the SiPM) of 1 or 2 V, false events clearly compete with true counts and the SPC pattern goes quite distorted, in a Gauss-type distribution with very bad resolution for the peaks. So, for getting clear patterns it is convenient to use a SiPM biasing voltage not so high (excess voltage below 1 V), not too short pulses (e.g.: between 4–10 ns), exciting pulse amplitude as low as possible and enough gain factor but not extremely large (for avoiding restrictions in dynamic range).

Figure 8 shows two important facts. In the first place, that

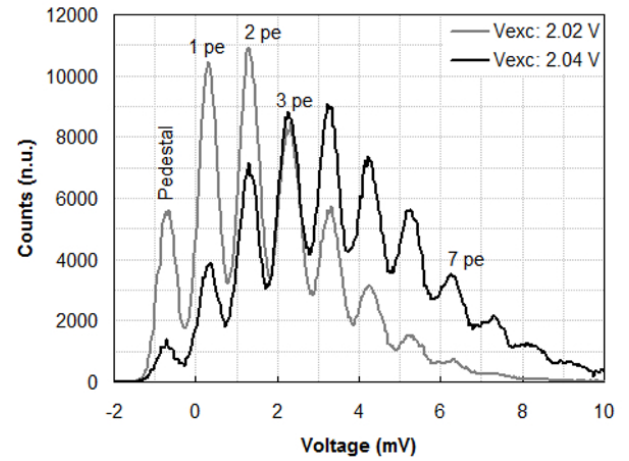


FIG. 6 SPC pattern obtained when reflectometric shortening system is used (short circuited coaxial stub length: 52 cm) with low gain in the preceding chain (16 dB). SiPM model S10362-33-100C (3 mm x 3 mm). Biasing voltage: 70 V. Incoming excitation pulses with width of 10 ns, wavelength of 400 nm and pulse amplitude for black trace 1 % higher than amplitude for gray trace.

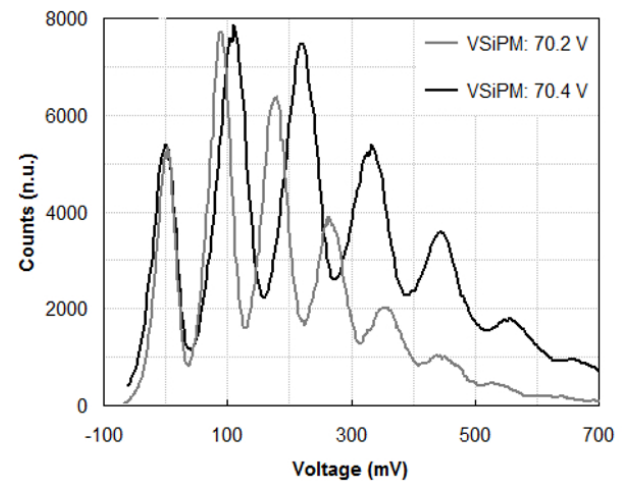
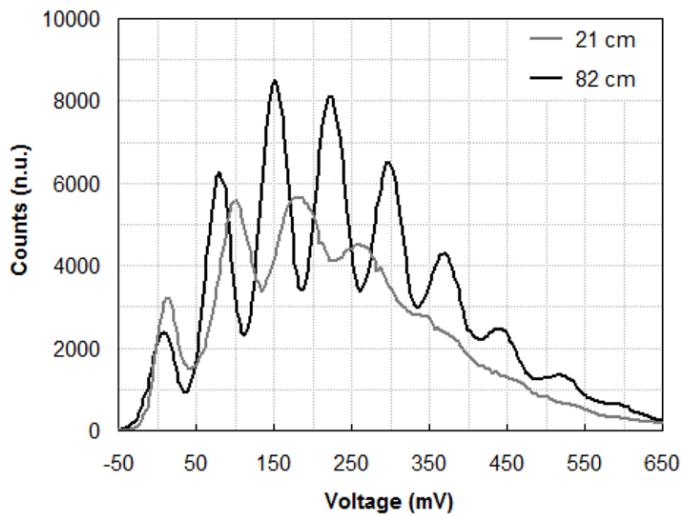
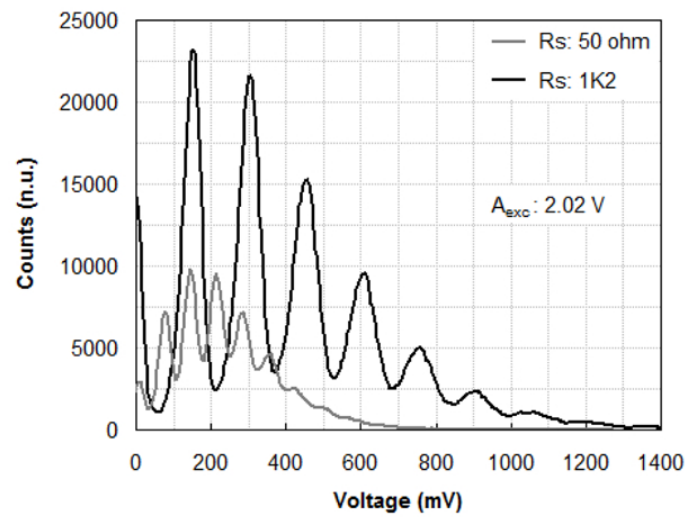


FIG. 7 SPC patterns obtained with reflectometric shortening system (short circuited coaxial stub length: 102 cm) showing the influence of biasing voltage. SiPM model S10362-33-100C (3 mm x 3 mm). Biasing voltage: 70.2 V (gray), 70.4 V (black). Incoming excitation pulses with width of 10 ns and wavelength of 400 nm.

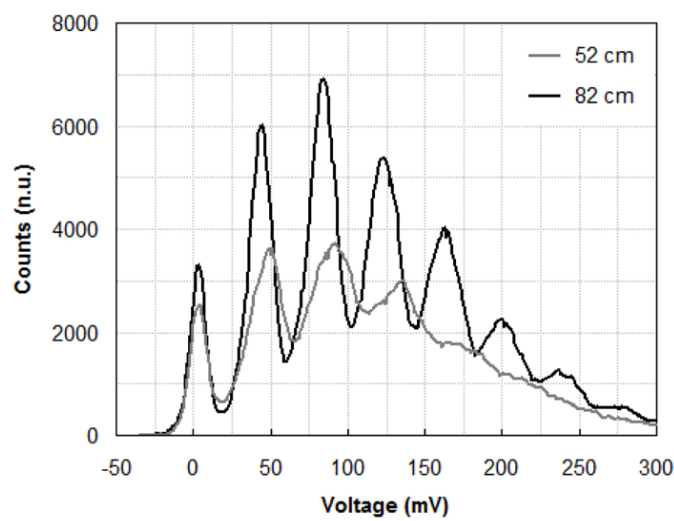
both shortening schemes (reflectometry based, Figure 8(a), and subtractor based, Figure 8(b)) are useful for getting sharp patterns. Subtractor based shortening scheme provides better defined peaks (higher relation peak-valley) with lower base corrupting distribution. However, pattern is shifted to lower voltages, which is a disadvantage. Nevertheless it could be corrected providing additional gain in the subtractor itself or as an additional final gain stage. But in that case, it would be necessary to check if resulting base distribution remains lower than the one obtained when reflectometric shortening scheme is used. In the second place, Figure 8 clearly shows that it exists an optimal length or an optimal range of lengths for the short-circuited stub in the reflectometric scheme and for the difference in length between the incoming inputs to the subtractor. When that length (or difference in length) is too short, detection pulses are shortened a lot, more than necessary, and a certain loss of the information that goes on the amplitude of photodetection peaks happens and consequently the SPC



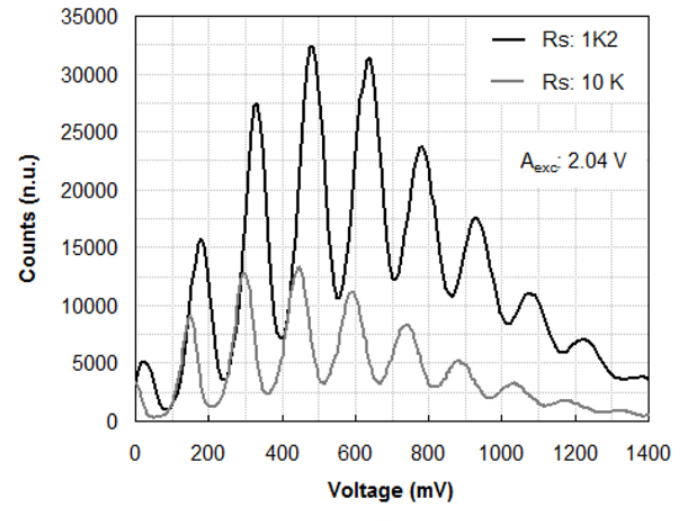
(a)



(a)



(b)



(b)

FIG. 8 (a) Influence of short-circuited stub length on SPC when reflectometry based shortening system is used. (b) Influence of difference in length between the incoming inputs to the subtractor on SPC when subtractor based shortening system is used. SiPM model S10362-33-100C (3 mm x 3 mm). Incoming excitation pulses with width of 10 ns and wavelength of 400 nm.

FIG. 9 Influence of sensing resistor value on SPC pattern. (a) Influence when resistor value is raised from a low value (50 ohm). (b) Influence when resistor value is raised from a medium value (1.2 kohm). Reflectometry based system, short-circuited coaxial stub length: 102 cm. SiPM model S10362-33-100C (3 mm x 3 mm). Biasing voltage: 70 V. Incoming excitation pulses with width of 10 ns and wavelength of 400 nm.

pattern is corrupted. On the contrary, when that length is excessive, pulses are needlessly wide and better definition of the pattern does not accompany that pulse stretching. Experimental results suggest that for SiPM model S10362-33-100C (3 mm x 3 mm) the optimal range of lengths, when coaxial lines are used, could be between 80 and 100 cm.

There are other factors that have influence on the SPC pattern. When exciting illumination wavelength is not near the maximum PDE of SiPM it is observed a reduction in the number of counts, and consequently, it is obtained a pattern with lower photopeaks and with higher pedestal (peak corresponding to zero photons). Nevertheless, counts and good SPC patterns were obtained even for exciting wavelengths quite far from central wavelength for detection (e.g.: for SiPM model S10362-33-100C, whose central wavelength is around 450 nm, sharp SPC patterns were obtained even with exciting wavelength of 800 nm). The exciting pulse repetition frequency is also a

parameter to be taken into account. According to the well-known degradation of photodetection signal as optical repetition frequency increases, the SPC pattern is also degraded accordingly: the number of photopeaks is lower, contribution of crosstalk is more important and peaks are wider and worst defined. Capacitor on SiPM cathode has a great influence on the SPC pattern. Although its value is not so important (good and comparable patterns were obtained for values ranging from 47 nF to 300 nF) its presence or absence is a critical issue. Only when this capacitor is acting on cathode and shortening is used it is possible to obtain correct SPC patterns (if not, pseudo-Gauss distribution with no distinguishable peaks are obtained). These two elements provide together a transformation in photodetection amplitude modulation, in such a way that amplitudes corresponding to a certain number of photons are now confined to a range better separated from neighbours. Also, sensing resistor plays an important role. As it is shown in Figure 9(a), when sensing resistor value increases moderately starting from a low value, enhancement of SPC pattern

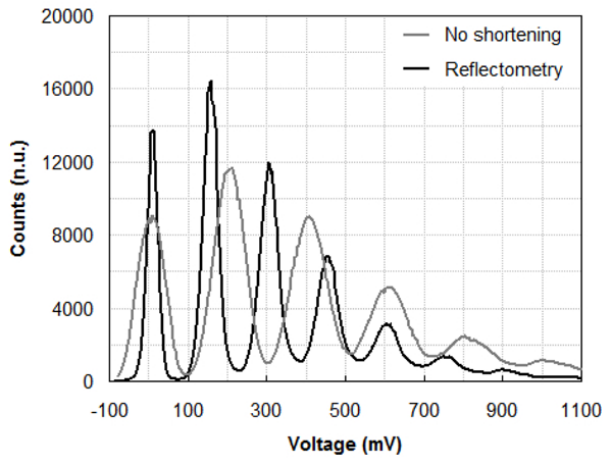
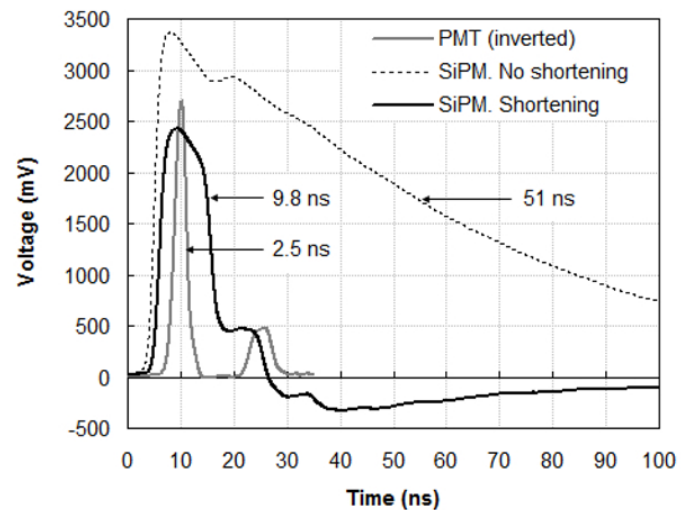


FIG. 10 Improvements on behavior are obtained using the shortening system even with SiPM of small active area. Comparing SPC obtained when no shortening is used (gray) and when reflectometric shortening scheme is used (black, short-circuited coaxial stub length: 52 cm). SiPM model S10362-11-050C (1 mm x 1 mm). Biasing voltage: 71.8 V. Incoming excitation pulses with width of 6 ns and wavelength of 650 nm.

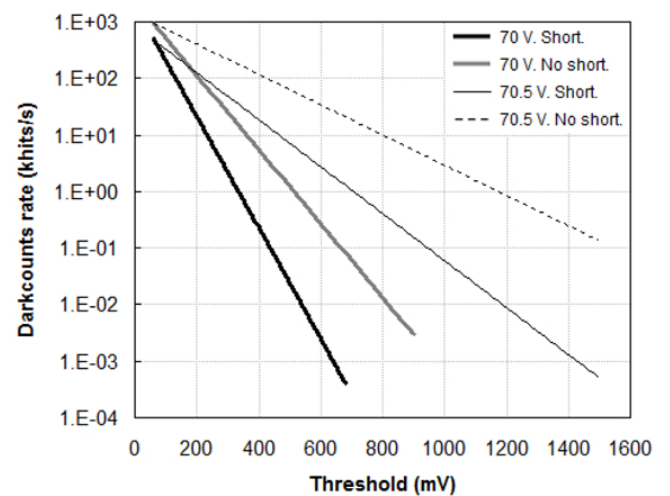
is evident. However, it is not possible to affirm that as higher the value of sensing resistor better the pattern definition. On the contrary, when sensing resistor increases a lot, pattern suffers a contraction (Figure 9(b)). So, sensing resistor and different capacitors implicated in the first stage of detection (cathode capacitor, output blocking capacitor, intrinsic SiPM capacitances) provide a frequency range that must be taken into account for enhancing single photon counting experiments.

SiPMs with small active area are not so influenced by crosstalk and it is possible to obtain well-defined SPC patterns only through amplification. Figure 10-gray shows a pattern obtained with SiPM model S10362-11-050C (1 mm x 1 mm). Shortening is not essential in that case, but as it can be observed in Figure 10, its use even with small area SiPMs is suitable: peaks are narrower and their enhanced heights allow better resolution between  $n$  and  $n \pm 1$  photons.

The advantage of using shortening is evident when large active area devices are used (compare Figure 4 and Figure 9). These devices could be especially interesting for applications in which it is necessary to cover a relatively large detection area with the lowest number of photodetectors as possible (e.g.: for detection in telescopes oriented to astroparticles like CTA). Devices that have been used traditionally for low intensity light detection (e.g.: Cherenkov telescopes, fluorescence spectroscopy, etc.) are photomultiplier tubes. These devices provide very short detection pulses (around 2–3 ns) and they are not so much influenced by darkcounts. However, they have also several drawbacks: big size, fragility, high voltage for operation (around 1000 V), danger of damage when accidental illumination happens, strong influence of magnetic fields that limits their applicability in several fields, etc. SiPMs, on the contrary, are little and robust devices, immune to magnetic fields, require low bias voltage (< 100 V) and are easy for manipulation and for making matrix ensembles. Main drawbacks of SiPMs are the great influence of darkcounts (due to its semiconductor nature) and the slow photodetection pulse falling edge. Shortening is able to reduce



(a)



(b)

FIG. 11 (a) Shortening allows to obtain a SiPM detection pulse comparable with the one provided by PMT. PMT model R10408. SiPM model S10362-33-100C (3 mm x 3 mm). PMT biasing voltage: 1200 V. SiPM biasing voltage: 70 V. Reflectometry based shortening with short-circuited coaxial stub length: 102 cm. Incoming excitation pulses with width of 10 ns and wavelength of 400 nm. (b) Shortening is able to reduce the influence of darkcounts when using SiPM. For every threshold, darkcounts were registered during 10 seconds using a time window of 80 microseconds. SiPM model S10362-33-100C (3 mm x 3 mm). With and without shortening (short-circuited coaxial stub length: 102 cm) for both biasing voltages: 70 V and 70.5 V. Nominal gain in amplification chain is 44 dB.

photodetection pulse width making it comparable with PMT pulse (see Figure 11(a)). PMT model used for this comparison was Hamamatsu R10408 [35] (spectral response from 185 nm to 650 nm, maximum quantum efficiency of 30 %, gain of  $4 \cdot 10^4$  and time responses below 3 ns). Furthermore, experimental results show that shortening also attenuates a lot the influence of darkcounts (Figure 11(b)). But, with no doubt, the main advantage when using SiPM is its ability for resolving photons. PMT is able to detect extremely low light intensities, but it is not possible to discriminate how many photons have arrived (Figure 12-gray). However, setting appropriate thresholds it is perfectly possible to perform this task when SiPM signal is shortened by mean of the strategies previously shown (Figure 12-black).

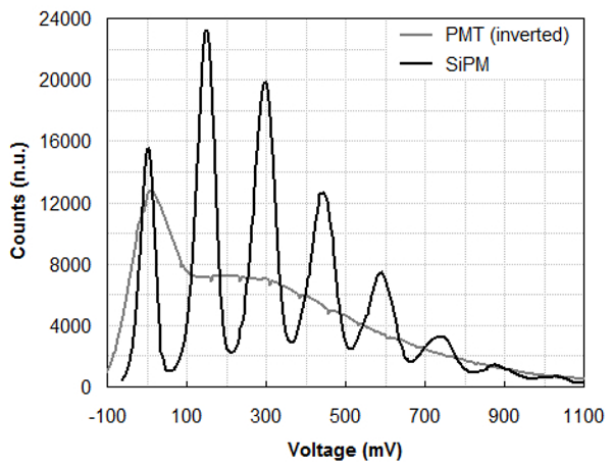


FIG. 12 Comparing SPC patterns obtained using Photomultiplier (PMT, gray) and Silicon Photomultiplier (SiPM, black) under the same conditions. PMT model R10408. SiPM model S10362-33-100C (3 mm x 3 mm). PMT biasing voltage: 1200 V. SiPM biasing voltage: 70 V. SiPM equipped with reflectometry based shortening (short-circuited coaxial stub length: 102 cm). Incoming excitation pulses with width of 10 ns and wavelength of 400 nm.

## 4 CONCLUSIONS

The experiments presented in this work show the usefulness of pulse shortening systems in the measurement of SPC patterns with large active area SiPMs. The advantage has been obtaining well defined SPC patterns, in a short time and using SiPMs that are not able to provide clear patterns working alone. Influence of several parameters on SPC patterns has been studied: incoming exciting pulse amplitude and wavelength, optical repetition frequency, SiPM biasing voltage, sensing resistor value, etc. It has been shown that it exists an optimal range of lengths for the short-circuited stub in the reflectometric scheme and for the difference in length between the two inputs to the subtractor in the subtractor based scheme which, for the SiPM used, could be located between 80 and 100 cm when coaxial lines are used. It was shown that, although the principal benefit is obtained for large active area SiPMs, shortening schemes also enhance small area SiPMs patterns. Finally, it was demonstrated one of the advantages of using SiPMs instead of PMTs. Shortening (using either reflectometric system or subtractor based system) can provide SiPM photodetection pulses as short as those provided by PMT and allows us to obtain real photon counting patterns. Both devices are able to detect very weak intensity illumination, but only SiPM is really able to discriminate the number of received photons. An important issue in this work is that all experiments and results were realized exciting SiPM with incoherent light, using for that cheap LED devices and feeding them with a digital functions generator. Although these shortening schemes do not reduce the dead time of photodetector, they are useful tools for conforming photodetection pulses for subsequent operations and for getting a set of thresholds for implementing single photon counters based on pulse amplitude detection. It is likely that shortening is also an appropriate pre-stage for feeding active quenching systems in order to enhance SiPM dead time.

## 5 ACKNOWLEDGEMENTS

This work has been funded by spanish MICINN Project FPA2010-22056-C06-04.

## References

- [1] D. Renker, "Geiger-mode avalanche photodiodes, history, properties and problems," *Nucl. Instrum. Meth. A* **567**, 48–56 (2006).
- [2] V. Kovaltchouk, G. Lolos, Z. Papandreou, and K. Wolbaum, "Comparison of a silicon photomultiplier to a traditional vacuum photomultiplier," *Nucl. Instrum. Meth. A* **538**, 408–415 (2005).
- [3] D. Renker, and E. Lorenz, "Advances in solid state photon detectors," *J. Instrum.* **4**, 04004 (2009).
- [4] J. Haba, "Status and perspectives of Pixelated Photon Detector (PPD)," *Nucl. Instrum. Meth. A* **595**, 154–160 (2008).
- [5] D. Renker, "New trends on photodetectors," *Nucl. Instrum. Meth. A* **571**, 1–6 (2007).
- [6] A. Stewart, E. Greene-O'Sullivan, D. Herbert, V. Saveliev, F. Quinlan, L. Wall, *et al*, "Study of the properties of new SPM detectors," *Proc. SPIE* **6119**, 61190A (2006).
- [7] J. P. Knemeyer, N. Marmé and J. D. Hoheisel, "Spectrally resolved fluorescence lifetime imaging microscopy (SFLIM)—an appropriate method for imaging single molecules in living cells," *Anal. Bioanal. Chem.* **387**, 37–40 (2007).
- [8] E. R. Tkaczyk, C. F. Zhong, J. Y. Ye, A. Myc, T. Thomas, Z. Cao, *et al*, "In vivo monitoring of multiple circulating cell populations using two-photon flow cytometry," *Opt. Commun.* **281**, 888–894 (2008).
- [9] D. J. Herbert, S. Moehrs, N. D'Ascenzo, N. Belcari, A. Del Guerra, F. Morsani, and V. Saveliev, "The Silicon Photomultiplier for application to high-resolution Positron Emission Tomography," *Nucl. Instrum. Meth. A* **573**, 84–87 (2007).
- [10] A. Braem, E. Chesi, C. Joram, A. Rudge, J. Seguinot, P. Weilhammer, *et al*, "Wave length shifter strips and G-APD arrays for the read-out of the z-coordinate in axial PET modules," *Nucl. Instrum. Meth. A* **586**, 300–308 (2008).
- [11] B. J. Pichler, H. F. Wehrl, A. Kolb, and M. S. Judenhofer, "Positron Emission Tomography / Magnetic Resonance Imaging: The Next Generation of Multimodality Imaging?," *Semin. Nucl. Med.* **38**, 199–208 (2008).
- [12] P. J. Clarke, R. J. Collins, P. A. Hiskett, M. J. García-Martínez, N. J. Krichel, A. McCarthy, *et al*, "Analysis of detector performance in a gigahertz clock rate quantum key distribution system," *New. J. Phys.* **13**, 075008 (2011).
- [13] M. Teshima, B. Dolgoshein, R. Mirzoyan, J. Nincovic, and E. Popova, "SiPM development for Astroparticle Physics Applications," *Proc 30<sup>th</sup> Int. Cosmic Ray Conf.* **5**, 985–988 (2007).
- [14] R. Mirzoyan, B. Dolgoshein, P. Holl, S. Klemin, C. Merck, H. Moser, *et al*, "SiPM and ADD as advanced detectors for astro-particle physics," *Nucl. Instrum. Meth. A* **572**, 493–494 (2007).
- [15] N. Otte, "The Silicon Photomultiplier—A new device for High Energy Physics, Astroparticle Physics, Industrial and Medical Applications," in *Proceedings to SNIC symposium* (SLAC, Stanford, 2006).
- [16] N. Otte, B. Dolgoshein, J. Hose, S. Klemin, E. Lorenz, R. Mirzoyan, E. Popova, and M. Teshima, "The Potential of SiPM as Photon Detector in Astroparticle Physics Experiments like MAGIC and EUSO," *Nucl. Phys. B* **150**, 144–149 (2006).
- [17] F. Risigo, A. Bulgheroni, M. Caccia, C. Cappellini, V. Chmill,

- N. Fedyushkina, *et al.*, "SiPM technology applied to radiation sensor development," *Nucl. Instrum. Meth. A* **607**, 75–77 (2009).
- [18] S. Vinogradov, T. Vinogradova, V. Shubin, D. Shushakov, and K. Sitarsky, "Efficiency of Solid State Photomultipliers in Photon Number Resolution," *IEEE T. Nucl. Sci.* **58**, 9–16 (2011).
- [19] M. Ramilli, A. Allevi, V. Chmill, M. Bondani, M. Caccia, and A. Andreoni, "Photon-number statistics with silicon photomultipliers," *J. Opt. Soc. Am. B* **27**, 852–862 (2010).
- [20] Z. Sadygov, A. Olshevski, I. Chirikov, I. Zheleznykh, and A. Novikov, "Three advanced designs of micro-pixel avalanche photodiodes: Their present status, maximum possibilities and limitations," *Nucl. Instrum. Meth. A* **567**, 70–73 (2006).
- [21] [http://sales.hamamatsu.com/assets/pdf/parts\\_S/s10362-33series\\_kapd1023e05.pdf](http://sales.hamamatsu.com/assets/pdf/parts_S/s10362-33series_kapd1023e05.pdf)
- [22] [http://sales.hamamatsu.com/assets/applications/SSD/Characteristics\\_and\\_use\\_of\\_SI\\_APD.pdf](http://sales.hamamatsu.com/assets/applications/SSD/Characteristics_and_use_of_SI_APD.pdf)
- [23] [http://sales.hamamatsu.com/assets/pdf/parts\\_S/s10362-11series\\_kapd1022e05.pdf](http://sales.hamamatsu.com/assets/pdf/parts_S/s10362-11series_kapd1022e05.pdf)
- [24] <http://www.keithley.com/data?asset=10756>
- [25] [http://common.leocom.jp/datasheets/153506\\_9741.pdf](http://common.leocom.jp/datasheets/153506_9741.pdf)
- [26] [http://www.lasercomponents.com/fileadmin/user\\_upload/home/Datasheets/divers-vis/ari/655nm/adl-65074tr.pdf](http://www.lasercomponents.com/fileadmin/user_upload/home/Datasheets/divers-vis/ari/655nm/adl-65074tr.pdf)
- [27] [http://www.datasheetcatalog.org/datasheet/infineon/1-bga616\\_1.pdf](http://www.datasheetcatalog.org/datasheet/infineon/1-bga616_1.pdf)
- [28] P. Antoranz, I. Vegas, and J. M. Miranda, "A 4 V, ns-range pulse generator for the test of Cherenkov Telescopes readout electronics," *Nucl. Instrum. Meth. A* **620**, 456–461 (2010).
- [29] P. Antoranz, *Contributions to the high frequency electronics of MAGIC II Gamma Ray Telescope* (PhD thesis, Universidad Complutense de Madrid, 2009).
- [30] <http://www.minicircuits.com/pdfs/ZPUL-21.pdf>
- [31] <http://www.minicircuits.com/pdfs/ZPUL-30P.pdf>
- [32] <http://www.national.com/ds/LM/LM7171.pdf>
- [33] [http://www.nxp.com/documents/data\\_sheet/BAT17.pdf](http://www.nxp.com/documents/data_sheet/BAT17.pdf)
- [34] <http://cp.literature.agilent.com/litweb/pdf/5989-5811EN.pdf>
- [35] [http://www.mpp.mpg.de/~haberer/projects/MAGIC/misc/photo\\_multiplier/hamamatsu\\_specs/02\\_R10408%20for%20MAGIC%20DATA%2020060824.pdf](http://www.mpp.mpg.de/~haberer/projects/MAGIC/misc/photo_multiplier/hamamatsu_specs/02_R10408%20for%20MAGIC%20DATA%2020060824.pdf)